AFRL-RZ-WP-TR-2007-2147

X-RAY 3D METROLOGY SYSTEM FOR SOFC DEVELOPMENT

Dr. Steve Wang

Xradia, Inc.

OCTOBER 2007

THIS IS A SMALL BUSINESS INNOVATION RESEARCH (SBIR) PHASE I REPORT.

AIR FORCE RESEARCH LABORATORY
PROPULSION DIRECTORATE
WRIGHT-PATTERSON AIR FORCE BASE, OH 45433-7251
AIR FORCE MATERIEL COMMAND
UNITED STATES AIR FORCE

NOTICE AND SIGNATURE PAGE

*//Signature//
THOMAS L. REITZ, Ph.D.
Chemical Engineer
Electrochemistry & Thermal Sciences

//Signature//
THOMAS L. REITZ, Ph.D.
Chief
Electrochemistry & Thermal Sciences

//Signature//
KIRK L. YERKES, Ph.D.
Deputy for Science
Power Division

REPORT DOCUMENTATION PAGE

Form Approved
OMB No. 0704-0188

The public reporting burden for this collection of information is estimated to average 1 hour per response, including the time for reviewing instructions, searching existing data sources, searching existing data sources, gathering and maintaining the data needed, and completing and reviewing the collection of information. Send comments regarding this burden estimate or any other aspect of this collection of information, including suggestions for reducing this burden, to Department of Defense, Washington Headquarters Services, Directorate for Information Operations and Reports (0704-0188), 1215 Jefferson Davis Highway, Suite 1204, Arlington, VA 22202-4302. Respondents should be aware that notwithstanding any other provision of law, no person shall be subject to any penalty for failing to comply with a collection of information if it does not display a currently valid OMB control number. **PLEASE DO NOT RETURN YOUR FORM TO THE ABOVE ADDRESS**.

1. REPORT DATE *(DD-MM-YY)*	2. REPORT TYPE	3. DATES COVERED *(From - To)*
October 2007	Final	27 February 2007 – 01 October 2007

4. TITLE AND SUBTITLE	5a. CONTRACT NUMBER
X-RAY 3D METROLOGY SYSTEM FOR SOFC DEVELOPMENT	FA8650-07-M-2706
	5b. GRANT NUMBER
	5c. PROGRAM ELEMENT NUMBER 65502D

6. AUTHOR(S)	5d. PROJECT NUMBER
Dr. Steve Wang	0605
	5e. TASK NUMBER PP
	5f. WORK UNIT NUMBER 0605PP13

7. PERFORMING ORGANIZATION NAME(S) AND ADDRESS(ES)	8. PERFORMING ORGANIZATION REPORT NUMBER
Xradia, Inc. 5052 Commercial Way Concord, CA 94520	

9. SPONSORING/MONITORING AGENCY NAME(S) AND ADDRESS(ES)	10. SPONSORING/MONITORING AGENCY ACRONYM(S)
Air Force Research Laboratory Propulsion Directorate Wright-Patterson Air Force Base, OH 45433-7251 Air Force Materiel Command United States Air Force	AFRL/RZPS
	11. SPONSORING/MONITORING AGENCY REPORT NUMBER(S) AFRL-RZ-WP-TR-2007-2147

12. DISTRIBUTION/AVAILABILITY STATEMENT
Approved for public release; distribution unlimited.

13. SUPPLEMENTARY NOTES
This is a Small Business Innovation Research (SBIR) Phase I Report. (SBIR rights waived; waiver letter on file.)

Report contains color.

PAO Case Number: WPAFB 07-0553, 28 Nov 2007.

14. ABSTRACT
Report developed under a SBIR contract.

This SBIR project sought to develop an x-ray system for nondestructively imaging the internal three-dimensional structure of solid oxide fuel cells (SOFC) – a CT scanner for fuel cells with sub-50 nm resolution. During the Phase I project, Xradia completed two key tasks that demonstrate the use of this technology in routine SOFC development, specifically for studying Sulfur contamination.

15. SUBJECT TERMS
SBIR Report, Sulfur Tolerance, SOFCs, military logistic fuels, X-ray metrology

16. SECURITY CLASSIFICATION OF:			17. LIMITATION OF ABSTRACT:	18. NUMBER OF PAGES	19a. NAME OF RESPONSIBLE PERSON *(Monitor)*
a. REPORT Unclassified	**b. ABSTRACT** Unclassified	**c. THIS PAGE** Unclassified	SAR	20	Thomas L. Reitz **19b. TELEPHONE NUMBER** *(Include Area Code)* (937) 255-4275

Standard Form 298 (Rev. 8-98)
Prescribed by ANSI Std. Z39-18

Table of Content

A. Significance and Public Benefit

The key benefit brought by the proposed instrument is the unique capability to directly study the detailed three-dimensional structure of the TPB in a SOFC at tens of nm resolution, non-destructively and dynamically while the device is in operation. Since most performance degradations can be traced to the loss of the interaction length in the TPB, understanding how it's affected by fabrication and operation parameters is among the most critical aspect in the development of practical fuel cells. The introduction of this tool therefore provides a new powerful technique for understanding the performance of SOFC and its aging mechanism, as well as improving the fabrication techniques and optimizing the operation conditions that is far more effective than the traditional electron and visible light microscopy techniques. It therefore has the potential to accelerate the development of the SOFC technology and reduce the time to market. At the same time, it would make the development of SOFC technology more efficient and cost-effective by providing faster and more accurate feedback to the researchers and developers.

Large-scale proliferation of practical SOFC power plants would have ground-breaking impact on our way of life. Most of the energy in the United States is supplied by fossil fuel burning power plants with 25-30% efficiency, and typical 25-40% transmission and conversion loss. This dependence on fossil fuel is particularly acute with the increasing global demand. An SOFC with combined electrical and thermal power efficiency of 80% could potentially reduce the energy need by factor of 2 to 3. SOFC technology therefore can significantly reduces the fuel payload requirement as well as thermal and chemical emission signatures of a vehicle, and without the need of exotic fuels. Furthermore, SOFC-based power generation has the potential for far-reaching impact on energy consumption and environmental conservation in the near future, particularly in the environment of increasing global oil demand and stability concerns with the production regions. In particular with SOFC, hydrogen fuel is not required as hydrocarbons can be reformed directly in the fuel cell. Hence there is no need to invest in additional fuel delivery and storage infrastructures. Consequently, the impact on society can be much more immediate than other fuel cell technologies.

The dramatically higher energy efficiency is also accompanied by much lower pollutant emission per unit of usable power, thus making fuel cells are also far more environmentally friendly than traditional power generation technologies. The US Fuel Cell Council concluded that the first fuel cell power plants developed by UTC Fuel Cells create less than 20 grams of pollutants per MWH compared to 11,388 grams per MWH for a traditional fossil-fuel burning plant.

Because of its great potential in energy conservation and environmental protection, the commercialization of fuel cell technology is among the most important product development undertaking in the world today. The market for stationary fuel cells is expected to grow to over 10 billion by 2010 and the overall market is expected to reach $95 billion by this time. What's more, besides the economic benefits, wide use of fuel cell technology would have far-reaching strategic and geo-political impacts by drastically reducing our overall dependence on fossil fuel.

B. Project Objectives and Motivations

This SBIR project aims to develop an x-ray imaging system for nondestructively imaging of internal three-dimensional structure of solid oxide fuel cells (SOFC) – a CT scanner for fuel cells with sub-50 nm resolution. During the Phase I project, we have complete two key tasks that demonstrate the use of this technology in *routine* SOFC development, specifically for studying Sulfur contamination:

1. Demonstrate the ability to routinely prepare a SOFC device for the imaging without affecting the operating functionalities. This requires thinning the region of interest to several hundred um using a "dimpling" technique perfected by the semiconductor industry.

2. Image the 3D structure of the region of interest and demonstrate the ability make measurement of the TPB from the data and sufficient throughput for dynamic studies.

These results (described in more detail in Section D) support a Phase II project to develop a fully functional system that is able to image the three-dimensional morphology of the most critical interaction region of a fuel cell sample nondestructively and automatically segment the 3D data to identify different material composition. This will allow researchers to monitor and analyze the structure of a fuel cell, possibly even in its operating conditions, and help understand failure mechanism to improve their reliability and performance.

Fuel cell devices convert chemical energy directly into electrical energy without combustion. Their immediate benefit is much higher energy conversion efficiency and the drastic reduction of pollutants. Solid-oxide fuel cells, in particular, are able to utilize existing widely used hydrocarbon fuel to simultaneously generate thermal and electrical power with combined heat and power (CHP) efficiency of over 80%. In contrast, internal-combustion engines (ICE) provide only up to 35% efficiency with most of the energy loss in the form of exhaust heat and pollution. SOFC technology can therefore significantly reduce the fuel payload requirement as well as thermal and chemical emission signatures of a vehicle, and do so without the need of exotic fuels. Furthermore, SOFC-based power generation has the potential for far-reaching impact on energy consumption, environmental conservation, and national security, particularly in the environment of increasing global oil demand and instability in the oil-producing regions.

A critical step in making these devices practical is developing electrode and electrolyte components with high efficiency and long life time against aging and contaminations. The electrochemical reactions occur in a narrow zone along the *three-phase boundary* (TPB), where the three reaction elements: cathode, solid electrolyte, and gas are in contact. Better electrochemical performances are expected for components with larger TPB length per unit area. Much of SOFC research and development efforts are therefore focused on producing nano-porous structures with maximum TPB length as well as optimizing operating conditions that lead to high performance and corrosion and contamination resistance (*e.g.* Sulfur). Therefore, it is critical for the development of SOFC to have a 3D imaging tool capable of imaging and measuring the size, distribution, and connectivity of the pores and channels in these nano-porous structures. Furthermore, it is particularly desirable to nondestructively study the dynamic changes of these structures *in-situ* and while the device is in operation.

The imaging techniques used today are primarily based on electron microscopy, which is capable of providing extreme high resolution but it is difficult or even impossible to image many important parameters for SOFC research, such as the connectivity of pores and channels. Because of the shallow penetration depth of electrons, the region of interest (ROI) must be mechanically cross-sectioned to reveal buried structures for imaging in both scanning electron and transmission electron microscopes. In addition to that the process is tedious and destructive, is also prone to introducing artifacts, and is particularly problematic with the hard porous materials used in fuel cells. Furthermore, it is difficult or even practically impossible to obtain a 3D image of the connectivity of the pores and channels, which is critical for SOFC research. The system we propose solves these problems by taking advantage of two fundamental benefits of x-ray microscopy: high penetration power and good high resolution. In addition, it also offers elemental sensitivity for 3D imaging of a specific element. The large penetration depth allows imaging through the ROI without the need of cross-sectioning. By using CT imaging techniques, the exact 3D structure of a sample can be obtained non-destructively even while the device is in operation. The strong dependence of x-ray absorption on material type provides the ability to distinguish the four major material types in a fuel cell: cathode, electrolyte, air, and low-Z contaminants such as Sulfur. This means that both morphology and composition of the TPB can be directly measured from the 3D images to understand a SOFC's electrochemical state and predict its performance. This provides a

powerful metrology capability that is extremely valuable for the development of fuel cells. By providing direct and relevant information on the exact operating conditions of the device, it has the potential to significantly reduce the development time and improve the reliability.
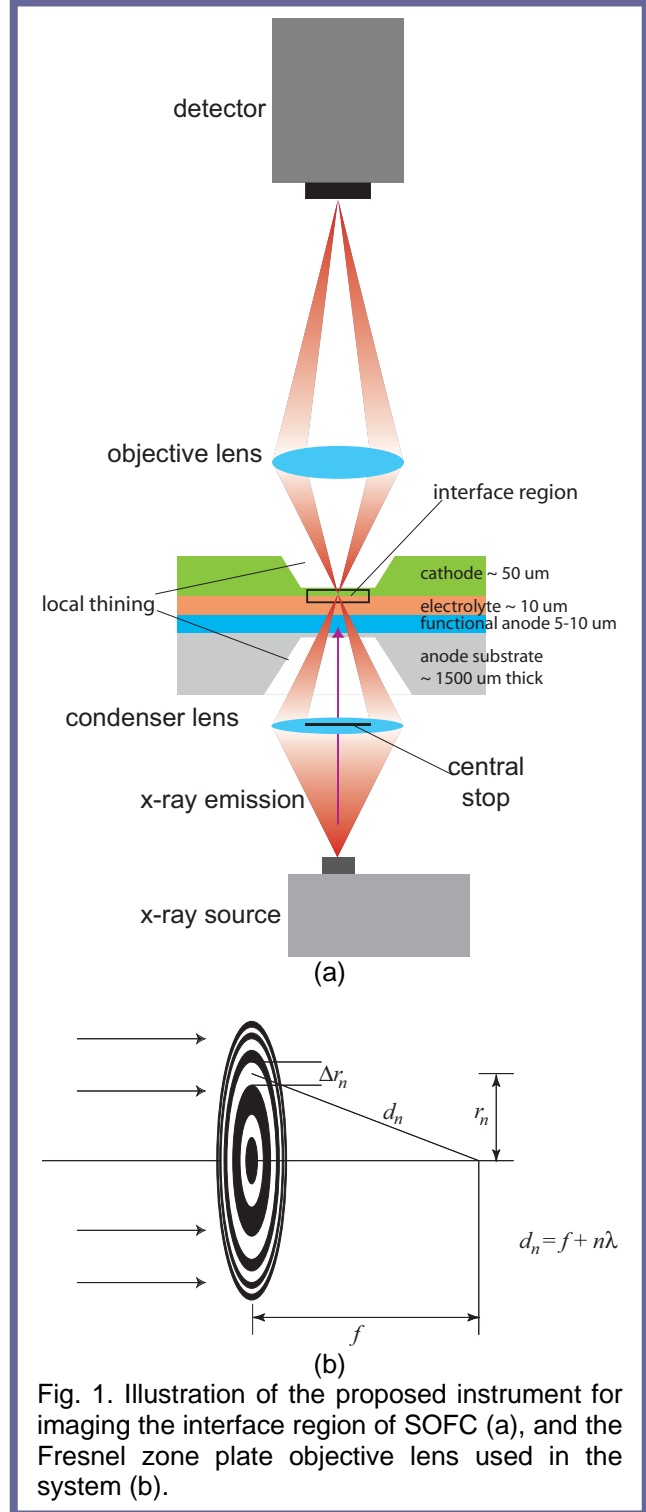
C. Technical Approach

The ultimate goal of the proposed tool is to develop a x-ray imaging based technique to nondestructively image the three-dimensional structure of the interface area of LSM/YSZ at 60 nm resolution while being able to distinguish four different materials: LSM, YSZ, Sulfur, and air (empty gap space). There are two important elements to this approach: (1) how to resolve the structures in 3D and (2) how to distinguish different materials. We will discuss them individually in more detail in this section.

C.1 Imaging System Configuration

To achieve the high resolution required for analyzing the TPB structure, we will use a transmission x-ray microscope (TXM) in a configuration shown in Fig. 1. In a setup similar to a conventional visible light microscope, it consists of an x-ray source, condenser lens, objective lens, and an area detector system. Such x-ray imaging systems were first developed at synchrotron radiation sources to serve the basic research community. Xradia has developed a table-top unit that has been adopted by semiconductor manufacturing companies for their failure analysis laboratories.

It is worth noting that the problem of imaging the TPB is also, to a large extent, shared among other nanotechnology and nano-electronics applications. For example, the failure analysis in semiconductor industries entails imaging the 3D circuit structure within a 10 um active area as the ROI, while with the SOFC, one must study the electrode-electrolyte interface with a thickness of a few um. We therefore expect this tool can be easily adopted for SOFC research and development applications.

In Xradia's system, the x-ray source will be a rotating anode type with Mo target to generate 17.5 keV x-ray radiation. The condenser will be a capillary reflective lens, and in order to achieve the 60 nm resolution a Fresnel zone plate lens will be used as the objective. A lens-coupled

Fig. 1. Illustration of the proposed instrument for imaging the interface region of SOFC (a), and the Fresnel zone plate objective lens used in the system (b).

3

scintillated CCD camera will be used as the detector. The 17.5 keV x-ray radiation allows samples with 100-200 um thickness to be imaged. This means the anode substrate of the SOFC needs to be thinned locally near the region of interest. This can be done with a mechanical process called *dimpling* that has been used routinely in semiconductor industries to remove the Si substrate while keeping the circuitry intact. Skilled operators can routinely use this technique to remove nearly all the substrate while leaving the active circuitry without damage the delicate interconnects. This sample preparation technique will be adopted during the project. *Note that this mechanical process does not reach the region of interest*. Instead, the materials are removed *around* the ROI, but leaving the active area intact, as shown in Fig. 1(a).

In order to observe dynamic changes of the TPB *in situ*, we will develop a experimental chamber that allows the SOFC device to operate normally and also allow the imaging x-ray beam to pass through. A schematic design is shown in Fig. 2. It is essentially a standard test chamber for planar SOFC devices modified with two x-ray windows. Such a test chamber typically contains seals to isolate the two sides of the device, gas feed-through tubes to inject and remove fuel air, and exhaust gases, heaters to starting the electrochemical reaction, electrodes to draw electric power, and other measuring devices. Starting with such an apparatus, we first cut two openings on both sides and weld in two cones shaped window made from a thin metallic or ceramic membrane. Since we are using hard x-ray radiation with 17.5 keV energy, we have a wide choice of window material with acceptable absorption. For example, 200 um thick sapphire (Al_2O_3) provides about 80% transmission and are commercially available.
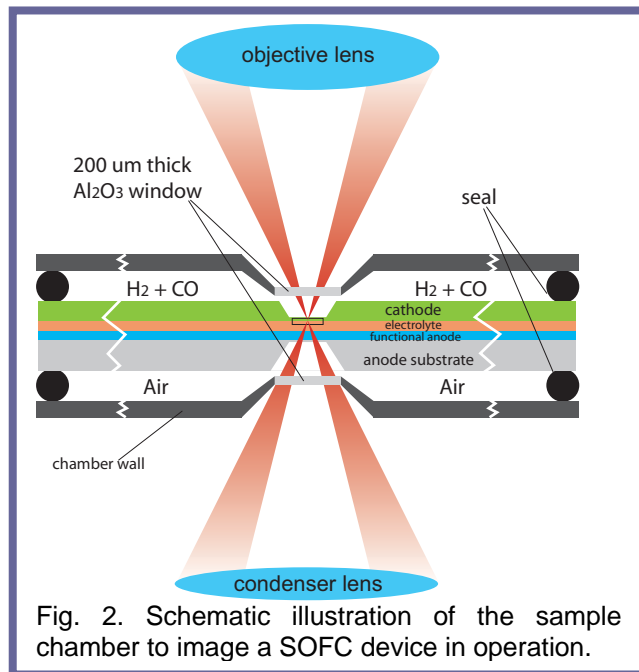

Fig. 2. Schematic illustration of the sample chamber to image a SOFC device in operation.

C.2 Zone Plate Objective Lens

The key component in the system shown in Fig 1(a) is the objective lens, a Fresnel zone plate. As illustrated in Fig. 1(b), a zone plate focuses electromagnetic radiation by diffraction, as opposed to the refraction effect used by glass lens for focusing visible light. It is essentially a circular diffraction grating with the grating period decreasing towards the periphery. With this arrangement, the diffraction angle increases with the increasing radius, and all radiation passing through the zone plate converges to a focal point. The diffraction-limited resolution of a zone plate measured by the Rayleigh criterion is simply 1.22 times the width of the outer-most grating line, or the *outermost zone width*. The focal length of a zone plate is expressed as $f = D\Delta r/\lambda$, where is D the diameter, Δr is the outer-most zone width, and λ is the wavelength. The numerical aperture is $NA = \lambda/2\Delta r$. From these properties, we see that the challenge of producing high-resolution zone plates lies in fabricating structures with extremely fine width. For example, in order to achieve the 60 nm resolution, we need to fabricate a zone plate lens with an outer most zone width of 50 nm.

The depth of field (DOF) is generally defined as twice the resolution divided by the numerical aperture. For our imaging system, this is about 200 um. Therefore a region of interest with 100-200 um is

contained completely within the DOF. In other words, all structures in the region of interest are imaged with 60 nm resolution and there is no defocus effect.

C.3 Resolving Structures in 3D

The volume of the ROI is a region with a few um thickness and extends over the area of the SOFC. One typically needs to image a 20 um × 20 um sample area per measurement. This problem is similar to that in semiconductor failure analysis applications, where one needs to identify broken or shorted interconnects in an integrated circuit (IC) chip. In their case, a similar sized volume in the IC, which has typically 10 um thickness and extends throughout the die, must be imaged non-destructively with a similar resolution. We will use a similar technique to study the 3D structures of the interface area between the cathode and the electrolyte, or the anode. The TPB is then identified from the 3D image and the effected interaction length can be measured.

We will use a computed tomography (CT) algorithm originally developed in the medical imaging community to resolve these features in depth. In the imaging system shown in Fig. 1, the x-ray beam passes through the sample to record an image containing all features that overlap in the depth direction. With tomography imaging process, the sample is imaged at different view angles to acquire a series of *tomographic projections*, and these projections are then mathematically backprojected into a volume data to form a 3D representation of the object. The features in the sample can then be analyzed by studying
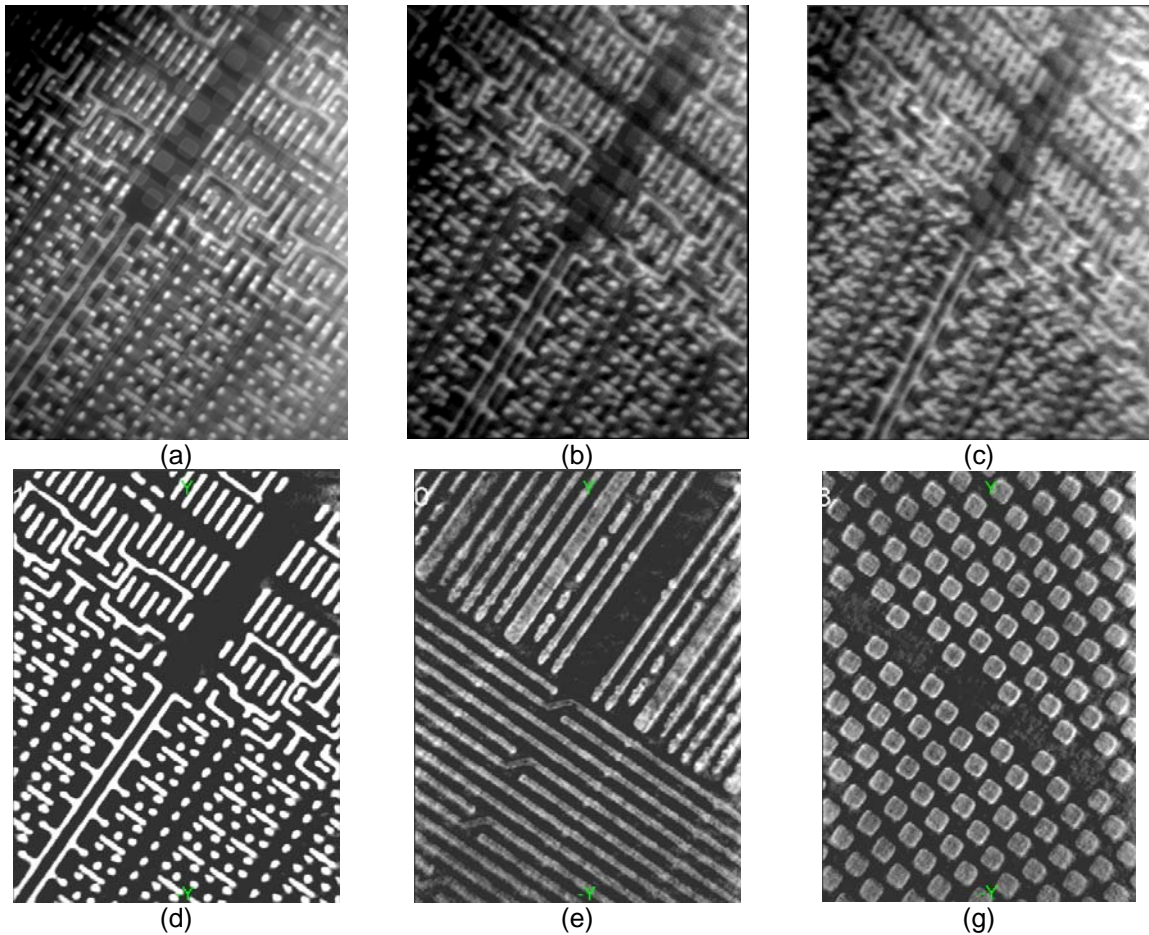

Figure 3. Illustration of 3D imaging with x-ray nano-tomography. Images (a)-(c) shows projectioins of the sample were acquired at different tilt angles at 60 nm resolution. Sections of reconstruction showing 3 of the 5 metal layers in (d-g) illustrate the ability to separate structures in space.

the data volume. Typical techniques used in the analysis include studying the cross-sectional views of the volume, or *virtual sectioning*, as is most often used in medical imaging applications, and studying the volume rendering. It's important to stress that this is done without physically modifying the object, while in contrast, to obtain equivalent cross-section views with SEM, one must physically cut and section the sample through the region of interest – a completely destructive process. In the medical imaging analogy, the TXM is compared with non-invasive imaging methods such as CT or MRI while SEM imaging can be compared to the invasive procedures such as biopsy or exploratory surgery. And their applications should comparable as well: the non-invasive imaging method should be used as the first screening or diagnosis procedure, while the invasive methods is applied with the non-invasive methods cannot provide a definite answer.

An example of this technique is shown in Fig. 3, where an integrated circuit sample was imaged at different tilt angles. Projections at 0°, 25°, and 45° are shown in Fig. 8(a-c). In these images, the resolution is about 60 nm, similar to the SEM images shown in Fig. 3(b) and 4, and the field of view is slightly larger than in the SEM images. After reconstruction the 3D structure of the sample, "*virtual sections*" of the volume data were extracted and shown in Fig. 8(d-e). Note that the overlapping circuit structure that are very difficult to interpret from the 2D projections 7(a-c) are clearly resolved in depth in the reconstruction images in Fig. 8(d-e). With the same method, the porous structures of a SOFC, with similar size as the IC interconnects, can be imaged in 3D. Important properties of the sample, including volume, surface area, linear distances, and density can be measured directly from the volume data. We expect to be able to use a similar volume data of a SOFC's TPB interface region to directly measure the interaction length.

3.3.4 Distinguishing different Materials

An important advantage of x-ray microscopy is that the absorption depends strongly on the elemental composition and x-ray energy. The way we can take advantage of this property to distinguish different materials can be summarized in Fig.4 where the $1/e$ attenuation lengths of LSM, YSZ, Sulfur, and air are plotted as a function of x-ray energy. Air is practically transparent with this combination of x-ray energy range and length scale. Note that the attenuation length for all three solid materials increase with the x-ray energy and the use of higher energy x-rays allows thicker sample to be imaged. For example, the images from the preliminary experiments were acquired using 8.05 keV x rays. This requires the sample to be thinned to about 20 um at the region of interest. But the instrument to be developed in the proposal will use 17.5 keV x rays from Mo emission, which will allow a region of interest to remain in 100-200 um thickness, thus greatly simplify the sample preparation process and furthermore allow observation at native operating conditions.

Figure 4. Plot of 1/e attenuation length of bulk LSM, YSZ, Sulfur, and air as a function of x-ray energy.

At 17.5 keV, the attenuation of LSM, YSZ, and Sulfur differ considerably. For example, with nearly half the attenuation

6

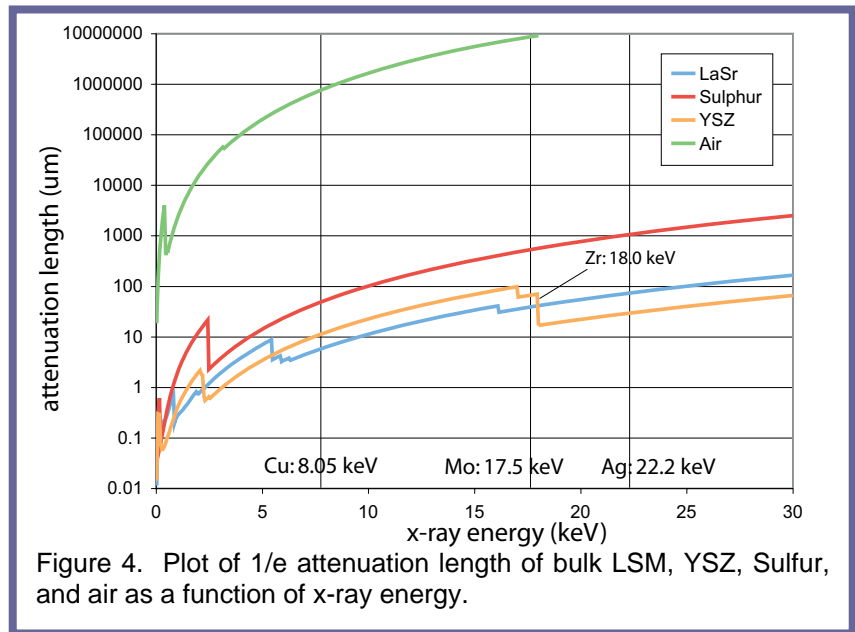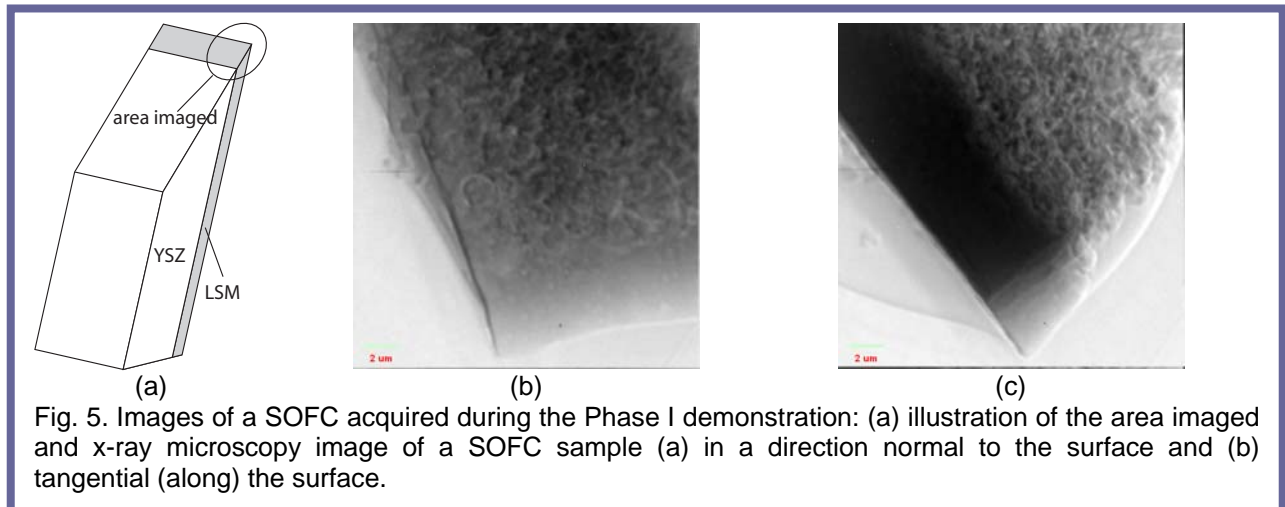length, LSM is more than twice more absorbing than YSZ, thus producing twice the image contrast. The two materials can then be identified in the 3D image from their very different absorptive properties, for example with a simple threshold. Air is practically transparent at this energy. It can be distinguished from both LSM and YSZ as empty space, while the solid materials can be distinguished from each other by their different pixel density. With this method, the three-dimensional structures of all three materials in the region where the electro-chemical reaction take place can be identified from a 3D image. This gives us the ability to study the TPB from the 3D data without physically altering the sample through destructive processes.

It is interesting to note that because of strong absorption edges of Y and Zr at 17.1 keV and 18 keV, there is actually a contrast reversal at x-ray energies above 18 keV. For example, at silver emission line at 22 keV, YSZ actually becomes about three times more absorbing than LSM. This means that when we take two images, one using a Mo source with 17.5 keV emission and one with Ag source with 22 keV emission, the YSZ material will appear more absorbing than LSM in the first image, but their contrast will reverse in the second image! We can take advantage of this property by using two x-ray source with these two target materials, and data obtained with their emissions are then combined to drastically increase the accuracy of the material identification. This differential absorption contrast technique has been used at synchrotron radiation-based microscopy facilities to map the elemental content of various samples with parts-per-thousand level sensitivity. This ability to map different materials in 3D will not only provide new and unique capability for studying the TPB of SOFC sample, it will also provide a powerful tool for materials science research in general. We will focus on developing the imaging system using 17.5 keV x rays during this project, but make provision for easily switching between two x-ray sources as future upgrades.

3.4 Feasibility Demonstration

We have performed a preliminary proof-of-principle experiment to demonstrate validity of the proposed concept. A planar SOFC sample was imaged with the a TXM at Xradia with sub-100 nm resolution and furthermore a tomographic data set was acquired. The results clearly demonstrate the ability to make detailed studies of the 3D structures of TPB non-destructively with sufficient resolution and furthermore, the potential to perform these studies dynamically while the device is in operation.

The TXM uses 8.05 keV x rays generated from a rotating anode x-ray source with Cu target. Its objective lens is a zone plate lens with 50 nm outer most zone width with theoretical maximum resolution of 60 nm. A scintillator coupled CCD camera with 1024×1024 pixels was used as the detector. The substrate of the SOFC sample was thinned to a wedge shape as shown in Fig. 5(a) with the region of interest

Fig. 5. Images of a SOFC acquired during the Phase I demonstration: (a) illustration of the area imaged and x-ray microscopy image of a SOFC sample (a) in a direction normal to the surface and (b) tangential (along) the surface.

marked. This procedure is needed because the attenuation length at Cu emission line is about 20 um. It is not necessary with the higher energy used in the proposed system. Image in Fig. 5(b) was acquired with the fuel cell layers perpendicular to the beam and 5(c) with the fuel cell tangential along the beam direction. Even though this energy was not optimized for this application, the difference in the absorption contrast between the LSM, YSZ, and open space is clearly observed in these images. The porous nature of the materials can also be readily observed.

The difference between TXM and electron microscopy techniques is also apparent. SEM images typically show only surface structure while the TXM image contains all features integrated through the sample along the imaging beam direction. These overlapping structures in fact make 2D x-ray images very difficult to interpret – as the medical imaging community realized decades ago and developed CT techniques to reconstructed the sample's 3D structures and therefore resolve the feature in depth.

We have also acquired a tomographic data set and reconstructed the 3D structure of the SOFC sample. Fig. 6 shows the cross-sectional views extracted from the volume data, with 4 slices along each of the 3 axis: (a-d) in the depth direction, where the slices are perpendicular to the imaging beam direction z; (e-h) in the rotation axis direction y (images parallel to the beam); and (i-l) along x axis perpendicular $y - z$ plane. The wonderful result is that the overlapping structures in Fig. 10 have been completely

Figure 6. The 3D volume data obtained with the SOFC sample shown in virtual cross-sectional views: (a-d) four slices in the different depth direction (perpendicular to imaging beam), (e-h) four slices along the rotation axis (parallel to beam), and (i-l) perpendicular to the previous axes.
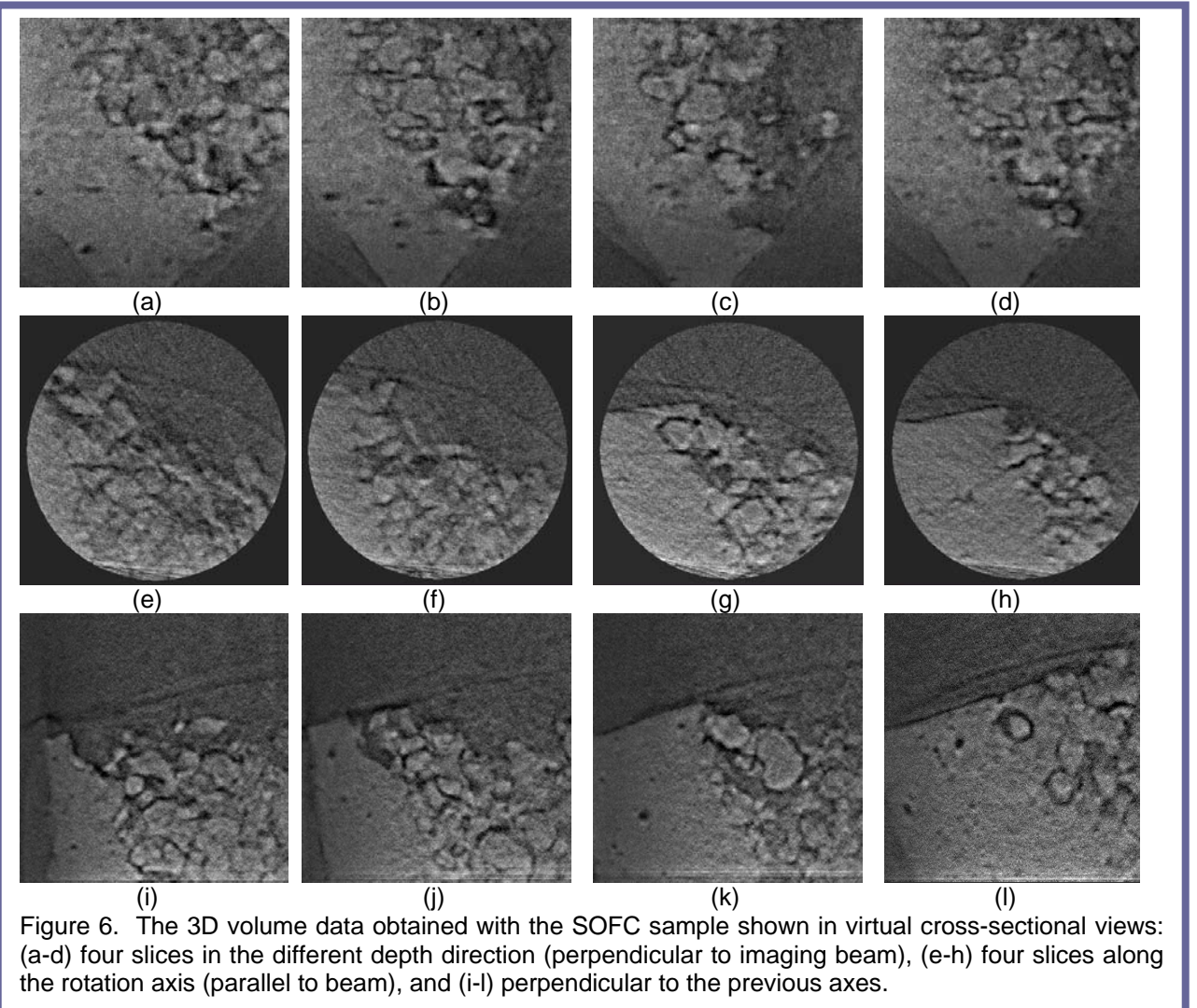
resolved in depth and the porous features of the sample can be understood clearly and measured exactly. The TPB can be easily identified from the image, and furthermore, the interaction length of the TPB can be measured from these images or from the 3D volume, perhaps automatically with specialized software. *This is in fact the most direct non-destructive measurement of the TPB that directly relates to the SOFC's performance characteristics*. Furthermore, since this measurement is made non-destructively and at about 2 cm stand-off working distance, it can also be made with a device in operation.

These preliminary results clearly demonstrate the validity of the proposal and its value to the SOFC research, development, and commercialization efforts. For the Phase II project, we will make several key improvement to develop a routinely used industrial tool:

1. The operating x-ray energy will be increased from 8 keV to 17.5 keV. Referring to Fig. 9, this will allow much thicker sample region of interest to be imaged. Samples can be locally thinned to 100-200 um at the ROI and this modification has little consequence its operation and performance, but leads to much easier sample preparation.
2. With improvement in the x-ray energy, optics and detector system, a factor of 4 gain in throughput can be expected. The preliminary data required 10 minutes per 2D image and the 3D data set took over 10 hours primarily due to the high sample absorption. With the proposed system, a complete 3D data set can be obtained in 2 hours. This is a times scale well-suited for monitoring the dynamic changes in the TPB structures.
3. Specialized 3D volume reconstruction tailored to the SOFC applications will be developed and automated measurement algorithms will be implemented to measure the total interaction length within the ROI from the volume data. Other quantitative measurements that predict the performance of the device, such as pore density and pore size distribution can also be automated.

D. Summary of Phase I Research Results

We have successfully completed the tasks proposed in the Phase I project with results meeting or exceeding the proposed objectives. These results demonstrated two critical abilities required to image the 3D structures of the three-phase boundary region in a SOFC sample, possibly even in its operating condition: (1) locally thin the sample with accurate depth and position control; and (2) image the 3D structure of the thinned sample and distinguish the anode, electrolyte, and cathode layers from the 3D images. Beyond these proposed tasks, we have performed spectral-microscopy imaging analysis that positively identified the sulfur contamination in spent SOFC devices provided by our program manager. Based on these encouraging results, we propose to develop a fully-functional prototype system in the Phase II project. We will first provide a report on the Phase I research and then the goals for the Phase II project.

D.1 Task 1: Developing Local Sample Thinning Techniques

The first task proposed in Phase I was to demonstrate the ability to routinely prepare a SOFC device for the imaging without affecting the operating functionalities. The x-ray energy used in this system is 8 keV which corresponds to tens of mms penetration depth in common materials found in fuel cells. A thick sample must therefore be thinned locally at the region of interest to perform x-ray imaging. It should be noted that 17.4 keV x-rays will used for the Phase II project providing significantly larger penetration depth, thus allowing nondestructive imaging of much thicker samples. Fig. 7 shows the cross-section of a SOFC sample with typical dimensions. In the particular sample, the cathode is about 16.5 mm thick. The electrolyte is the dense band with lowest porosity as shown in high magnification in Fig. 7(d). The functional anode can be clearly distinguished from the anode substrate by the porosity. The functional anode layer is about 25 μm in thickness and the substrate is about 650 μm thick. The thinning process should remove most of the anode substrate and the cathode, thus leaving about 10 μm of cathode layer, the complete electrolyte layer, and the functioning anode. The total thickness of the remaining region is
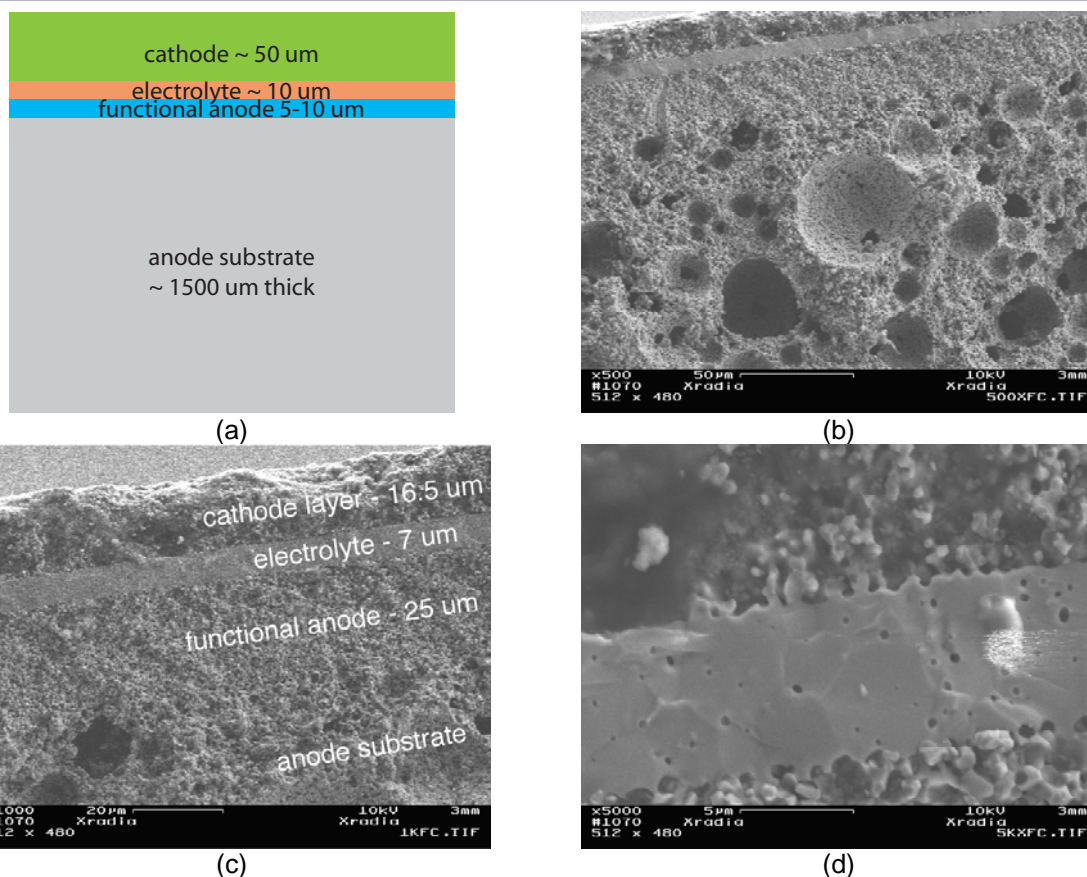
Figure 7. (a) Illustration of a SOFC layer structures. (b-d) Scanning electron micrographs of the cross-section of a SOFC sample shown with increasing magnification.

about 30 μm. *This thinning process will remove nearly all the local supporting material but does not affect the functional region of the fuel cell.*

We have developed a process that employs a "dimpling" technique developed by the semiconductor industry for the failure analysis of integrated circuit chips. Several commercial dimpling machines are available and we purchased one made by Allied High Tech Products, Inc. The dimpling mechanism uses a rotating grinding bit that also constantly rotates around the axis perpendicular to the sample plane. This action results in a hemispherical-shaped hole, as shown in Fig. 8. The machine has a micrometer controlled hard stop to control the cutting depth. By using a combination of mechanical depth gauge and optical microscope measurements, the dimpling depth can be controlled to several mm. In practice, the porosity difference between the anode substrate and functional anode is used as visual feedback. With practice of several runs, our process is able to routinely control the dimpling depth to 2-3 μm accuracy.

In our process, we first mark both sides of the region of interest with a home-made marking device that consists of two sharp pencil tips mounted on opposing sides of a outside measurement micrometer. We identify the ROI and position the micrometer on both sides. When the micrometer jaw closes, the pencil tips will mark the dimpling target area. We first dimple from the cathode side by up to 5-10 μm to leave about 5-10 μm of material. This depth is checked with a visible light microscope that has a depth resolution of about 1 mm. The sample is then turned over to dimple the anode side using the micrometer-controlled hard stop to control dimpling depth. When we roughly reach the functional anode, we begin to use visible light microscopy to check the porosity in order to identify the functional anode layer. This allows us to control exact depth around the layers of interest. It takes about 2 hours to dimple a typical
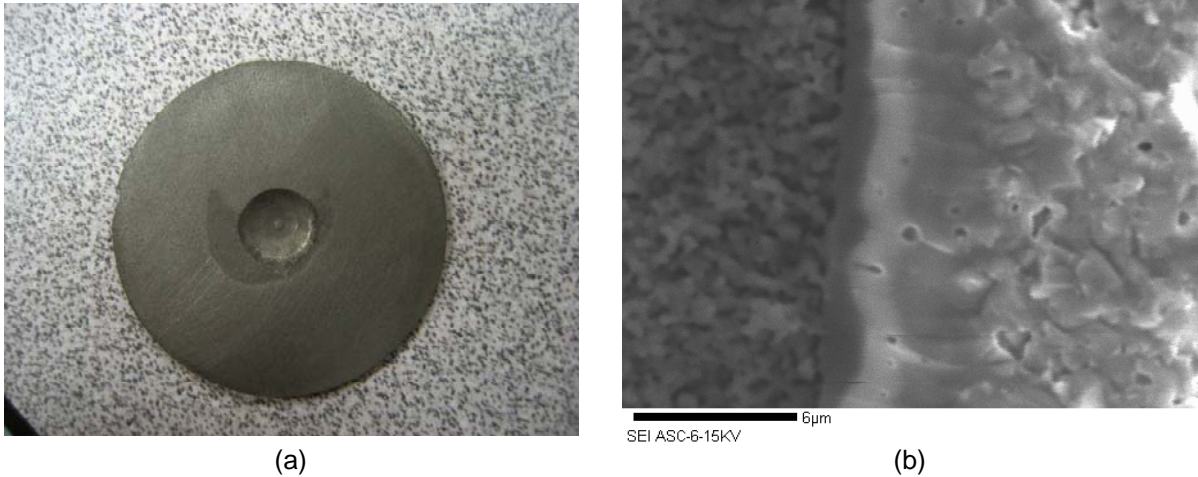
Figure 8. (a) A dimpled SOFC sample and (b) an SEM image near the region of interest showing the transition from the anode (left side), to elecryolyte, and to cathode.

disk-shaped sample with 650 ㎜ thick support anode substrate, with the dimpling machine running automatically for the most of the time and operator attention needed to confirm the depth position. The final depth can be verified with an outside micrometer gauge.

After the dimpling process, we quickly examine the sample with a scanning electron microscope (SEM) to check the quality of sample preparation. A typical image is shown in Fig. 8(b). In this sample, the anode side (left side in image) is highly porous with average pore size on the order of roughly a hundred nm to 1 μm. The cathode (right side) appears more dense with large but more sparsely distributed pores. The electrolyte between these two materials appears to be about 6.5 ㎜ thick. From this example, it is clear that the preparation process can preserve the fine structures of the SOFC with no observable damage at the resolution level of the SEM. The x-ray tool will go one step further to reveal a sample's internal structure as we demonstrate in the next section. This sample's ROI has been thinned to about 15 μm.

D.2 Task 2: Imaging Internal Structure at TPB

For the proof-of-principle demonstrations, we use commercial anode-supported fuel cells purchased from Fuel Cell Materials. The samples prepared with the dimpling process are mounted directly in our laboratory x-ray microscope to acquire the images required for 3D imaging, as will be described below. The microscope was optimized for imaging integrated circuit samples. It uses 8.05 keV x-ray radiation generated from a rotating-anode x-ray source with a Cu target. This energy is much lower than the 17.5 keV radiation planned for the Phase II system. The lower energy leads to about 5 times higher absorption so that the data acquisition time is about 25 times longer. For Phase I demonstration experiments we will use this system and extrapolate this exposure time factor for the Phase II system. The laboratory system has a resolution of 60 nm, slightly poorer than the Phase II system but is adequate for imaging the porous structure in the SOFC sample.

To image the 3D structure of the samples, we acquire projections with the sample tilted at different angles with respect to the beam axis (yaw angle in the aircraft convention). The planar nature of the sample prevent a full 360-degree rotation and we acquired projections within ±60 degree range in 2-degree steps. One such projection image is shown in Fig. 9(a). The features in this image are difficult to discern because the porous structures throughout the depth of the sample overlap. But these features can be resolved in depth with a computer tomography (CT) technique as used in medical imaging. These projections are mathematically assembled to generate the 3D structure of the fuel cell. using a filtered back-projection algorithm that is typically used in medical CT scanners The 3D data is shown in Fig. 9(b)
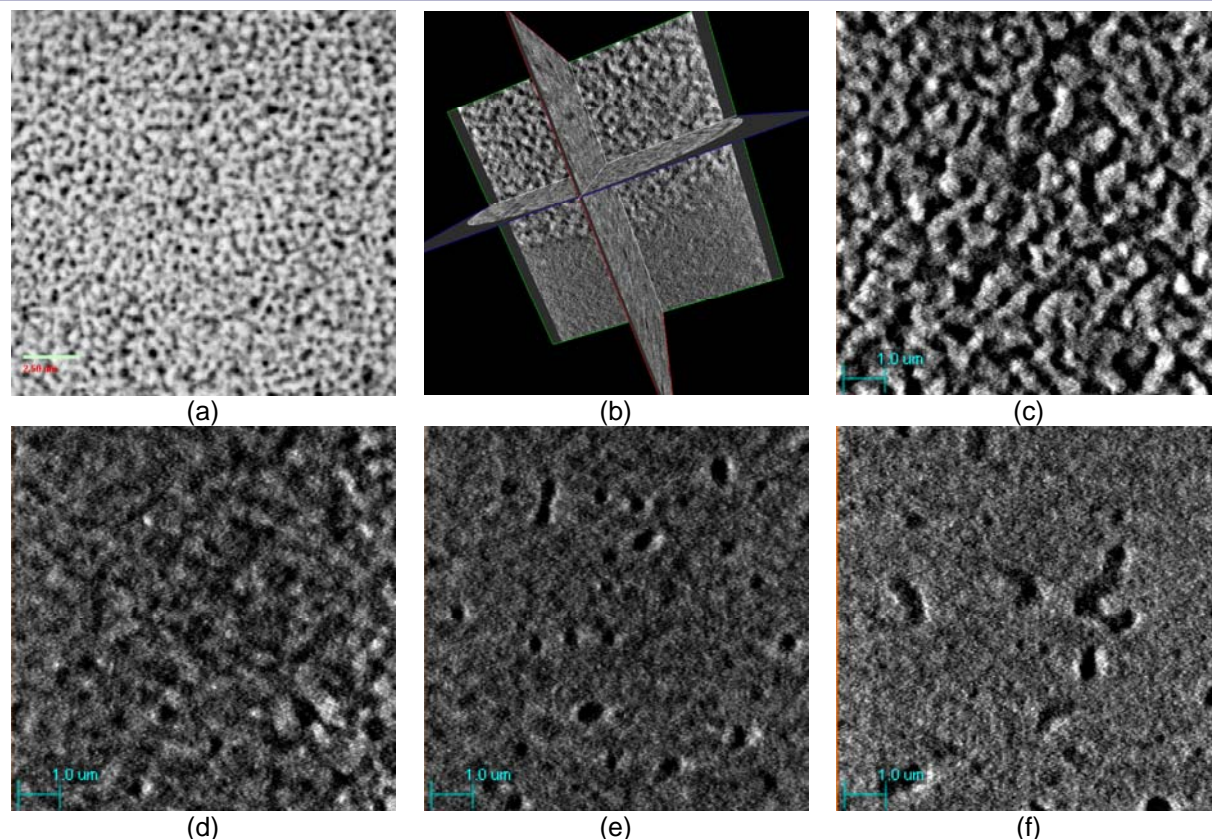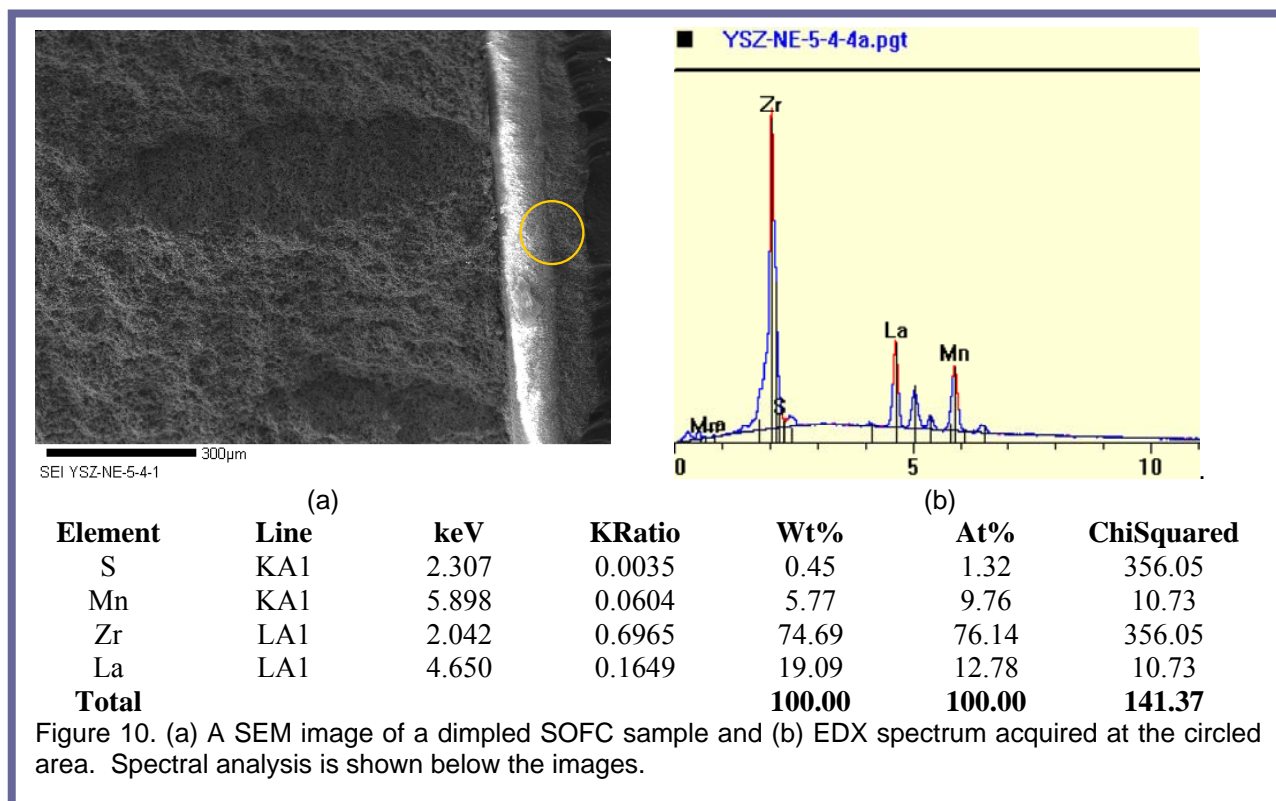
11

Figure 9. (a) A two-dimensional image of SOFC sample imaged through the cathode, electrolyte, and anode layers. The sample was dimpled with Xradia's process. (b) 3D cross-section view showing the transition from anode to electrolyte layers. (c) A virtual cross-section showing the anode layer, (d-e) transition between anode and electrolyte, and (f) electrolyte. Each layer has a thickness of 30 nm.

in an axial cross-section view and 4 additional cross-sections in the depth direction are shown in Fig. 9(c-f). In particular, Fig. 9(c) shows a cross-section in anode layers, Fig. 9(d-e) shows the transition between the anode and electrolyte, and Fig. 9(f) shows the electrolyte layer.

These x-ray images agree with the surface features SEM images shown in Fig. 8(b), but provide more important information on the internal structures in a non-invasive manner via virtual cross-sectioning. In order to observe the same features with an SEM, the sample must undergo a destructive mechanical cross-section process. Each projection image in this dataset has a pixel size of 30 nm, with 60 nm diffraction-limited resolution. This dataset contains 60 images and each projection image required 15 minutes, totaling 15 hours. This data acquisition time will be reduced to less than 3 hours with the Phase II system.

In additional to morphology, we have also performed elemental analysis with EDX to identify the sample's sulfur content and other contaminants. The SEM image is shown in Fig. 10(a) and the EDX spectrum performed at area B is shown in Fig. 10(b). The EDX analysis indicates there is about 1.32% of Sulfur by number of atoms (and 0.45% by weight). Because of this low concentration, the Sulfur contaminants are not visible in the x-ray image. However, contamination build up from extended use will be distinguishable with the Phase II system with improved resolution and material sensitivity.

Element	Line	keV	KRatio	Wt%	At%	ChiSquared
S	KA1	2.307	0.0035	0.45	1.32	356.05
Mn	KA1	5.898	0.0604	5.77	9.76	10.73
Zr	LA1	2.042	0.6965	74.69	76.14	356.05
La	LA1	4.650	0.1649	19.09	12.78	10.73
Total				**100.00**	**100.00**	**141.37**

Figure 10. (a) A SEM image of a dimpled SOFC sample and (b) EDX spectrum acquired at the circled area. Spectral analysis is shown below the images.

E. Summary

We have successfully completed the tasks proposed in the Phase I project with results meeting or exceeding the proposed objectives. These results demonstrated two critical abilities required to image the 3D structures of the three-phase boundary region in a SOFC sample, possibly even in its operating operation: (1) locally thin the sample with accurate depth and position control; and (2) image the 3D structure of the thinned sample and distinguish the anode, electrolyte, and cathode layers from the 3D images. Beyond these proposed tasks, we have performed spectral-microscopy imaging analysis that positively identified the sulfur contamination in spent SOFC devices provided by our program manager. Based on these encouraging results, we are optimistic about achieving the final goal of the first technology to be able to dynamically study the evolution of a SOFC's interaction region while it's operation. This system would provide an powerful capability to the development of practical fuel cell technology.